

MEASURES FOR GEOMETRIC RESOLUTION OF DIGITAL CAMERAS

Hans-Peter Bähr
Institut für Photogrammetrie und Fernerkundung
Universität Karlsruhe (TH)
Federal Republic of Germany
Commission I

1. Introduction

The resolving power of imaging systems has been a fascinating subject in photogrammetry since it exists. In the past 20 years scientific analysis came to understand the analog process as composed of subsystems, such as lens, film, forward motion and atmosphere. Mathematical treatment is feasible by taking into account the wave theory of the electromagnetic spectrum and by modelling the different components as Linear Time Invariant (LTI-) Systems (BAHR 1985). On the other hand, the geometric resolution of aerial photography always plays a central role in **practical and commercial** application of photogrammetry. This is shown e.g. by the efforts made in order to define common regulations for the calibration process.

Today, focussing the challenge of space platforms and digital systems, two mayor reasons require further activities in the field of geometric resolution:

- 1.) Mapping the earth's surface from space in competition to airborne methods
- 2.) Using digital cameras in competition to photographic cameras.

The two points coincide for spaceborne scanner systems.

Photographic cameras in space seemed a promising progress in the early 80s. Systematic efforts were made, particularly by the "Metric Camera Working Group" of ESA, in order to define the subsystems and to determine the image quality a priori (DUCHER 1985; KONECNY et al.1980; KONECNY et al.1982; SIEVERS, RUTHOTTO 1980; TOGLIATTI 1980). The results showed, that "Geometric Resolution" as a parameter of "Image Quality" is a very complex term and cannot be expressed by one value nor be reduced to one function.

The second point deals with a very immediate and urgent matter. Since scanner systems are in space, digital imagery is indeed intensively processed by photogrammetrists, but generally without direct comparison to analog photography (for an exception see KONECNY et al.1980). This situation has changed dramatically by a new generation of airborne scanner systems (HOFMANN 1986), but first of all by digital array cameras. As these systems might replace conventional photogrammetric cameras, a comparison of system performance is urgently needed.

However, well defined measures of geometric resolution like the Modulation Transfer Function (MTF) give no direct information about the real impact of image quality on a specific application.

For digital cameras, information like "pixel size" will turn out to be as inconvenient as "Lp/mm" for conventional cameras, and an MTF may contain only part of the information that the user needs to evaluate the resolving power of a digital camera system for his specific application. Therefore, measures like "pixel size" and MTF will be analysed together with **standard applications** like point determination by digital correlation and visual feature detection.

2. Digital Camera and Image Formation Process

FIG.1 shows the diagram of the used system. For image processing, a PDP 73/11 computer is available for standard applications, whereas PRIME machines may be taken for off-line operation (see paragr. 3.3).

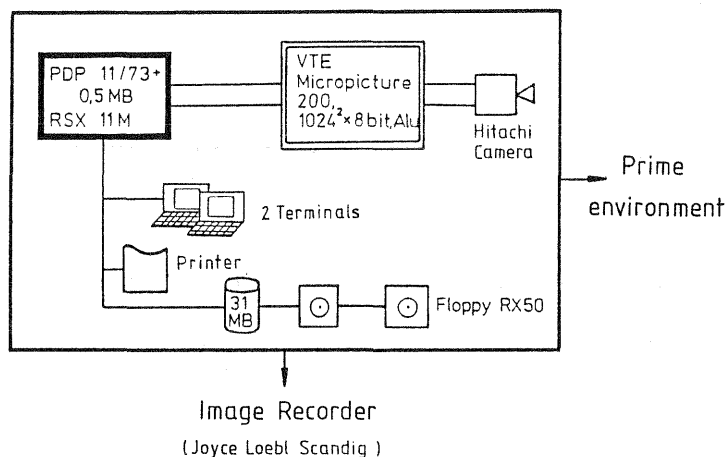


FIG. 1: Digital Camera and Image Processing System

In order to analyse the resolving power of the digital camera system, the process of image generation has to be thoroughly considered, especially with respect to the term "pixel element". The technical data of the video-system are given in Table 1.

Sensor area	8.8mm(h) x 6.6mm(v)
Number of sensor elements	388(h) x 577(v)
Size of sensor element	22.68 μ m(h) x 11.44 μ m(v)
Scanning time per line (CCIR standard, theoretical)	52.0 μ s
Digitizing frequency	15 MHZ
Digitizing time per pixel = 1/15 MHZ	66.67 ns
Scanning time per line (real, 66.67 ns x 512)	34.13 μ s
Effective sensor area, vertical (512/575)x6.6 mm =	5.877 mm
Effective sensor area, horizontal (34.13/52.0)x 8.8 mm =	5.776 mm
Size picture element, vertical 5.877 mm/512 =	11.48 μ m
Size picture element, horizontal 5.770 mm/512 =	11.28 μ m

Table 1: Pixel element size from system data
(see VÖGTLE, WIESEL 1986)

We have to recognize that the sensor element size in principle has nothing to do with the picture element size. This is due to the digitizing frequency (see Table 1), which converts the analog video signal output from the sensor cells into discrete steps of 66.67 ns. This sampling procedure reduces the horizontal sensor size from 22.58 μm to 11.28 μm pixel size.

Whereas in line direction pixels are separated by the digitizing process, separation between lines is done by a sync puls that defines a new line. The reliability of that pulse highly effects the geometric precision of the digital image (DÄHLER 1987). For the evaluation of image quality we have to regard, besides the above mentioned A/D conversion, the analog domain of the signal formation. Horizontal separation between sensor cells is done by vertical isolation, whereas for vertical separation alternating currents are used. Both means are not fully satisfactory: high contrasts result in irradiation, called "blooming" between lines and "tailing" in line direction.

The described image formation shows up as an extremely complex procedure. With regard to the resolving power of such a system we may draw the following conclusions:

- 1.) Both sensor element size and pixel element size give only approximate information about the geometric resolution of the system.
- 2.) According to the process of digital image formation, image quality will in principle differ for horizontal and vertical direction. This generates resolution which is depending on direction and not primarily on the position on the chip.

3. Applied Methods and Results

3.1 Direct Method from 3-Bar-Targets

This method is normally used for analysing the quality of aerial photography. In practice the resolving threshold is simply determined visually for high contrast. We may of course do the same for digital cameras. FIG.2 shows an image of 3-bar-targets. It is obvious, that the resolution in vertical direction, i.e. perpendicular to the sensor lines, is significantly better than in horizontal direction. This result was expected after paragraph 2. The example of FIG.2 refers exactly to the level, where the human eye considers the horizontal lines as still resolved, whereas the vertical lines are just below the resolution threshold. In relation to the respective sensor dimension, this resolution corresponds to

$$\frac{3\text{LP}}{13 \cdot 11.4 \cdot 10^{-3} \mu\text{m}} = 20 \text{ LP/mm (h)} \quad (1)$$

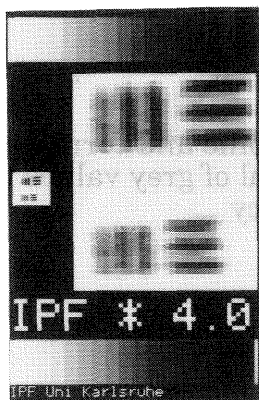


FIG. 2: 3-Bar-Targets at resolving threshold (1 Pixel = 100 μm)

Using the potential of the digital sensor, we may extend this simple method to get the Modulation Transfer Function (MTF), which contains more information about the resolving power than the representation in Lp/mm. The MTF is the quotient of output and input of the modulation signal for **all** frequencies involved in the signal:

$$MTF(f) = \frac{M_o(f)}{M_i(f)} = \frac{\frac{I'_{max} - I'_{min}}{I'_{max} + I'_{min}}}{\frac{I_{max} - I_{min}}{I_{max} + I_{min}}} \sim \frac{I'_{max} - I'_{min}}{I_{max} - I_{min}} \quad (2)$$

This simply equals $I'_{max} - I'_{min}$, if $I_{max} - I_{min}$ is set to 1 for frequency minimum.

This method has been used for determining LANDSAT-MSS MTF from microdensitometer measurements, too (BAHR 1979).

FIG.3 demonstrates the results for the digital camera system. The MTF shows a clearly better image quality in vertical direction than in horizontal direction, which was expected. If the contrast threshold for the human eye is assumed to be around 0.2, the corresponding values on the abscissa are 18 Lp/mm for horizontal and 26 Lp/mm for vertical direction, which confirms the result of (1). This corresponds to a proportion of 1,4 that still increases for higher contrast, e.g. 1.8 for $MTF = 0.5$ and 1.9 for $MTF = 0.7$. The original dimension of the sensor cells, being rectangular ($11.44 \mu\text{m}(v) \times 22.58 \mu\text{m}(h)$) therefore is still deductable from the MTF in spite of the quadratic pixel size of $11.48 \mu\text{m} \times 11.28 \mu\text{m}$.

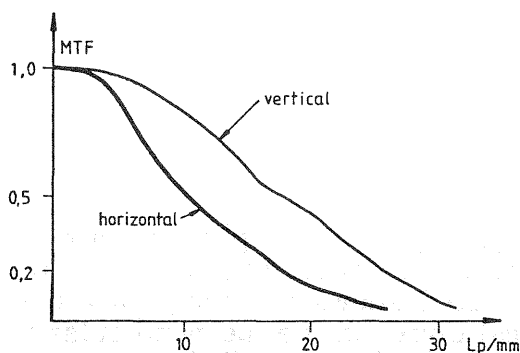


FIG. 3: MTF curves determined by the direct method

The measurement procedure for the direct method is rather time consuming. Even though the values in (1) are directly taken from the pixels by the computer, measurements have to be performed manually for many single frequencies. FIG.4 shows the respective result for one frequency. The MTF represents an objective result, obtained by digital measurements, whereas the determination of the resolving threshold includes subjective estimation. This is the case for both methods, i.e. if deriving the value Lp/mm directly from an image (FIG.2) or indirectly from the MTF (FIG.3)

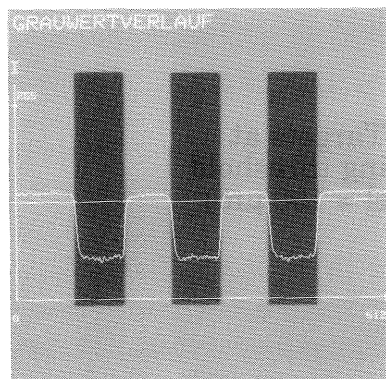


FIG. 4: Target profile and corresponding signal of grey values for 1 frequency

3.2 MTF from Edge Gradient Analysis (EGA)

The transformation of continuous spectral information is rigorously described by

$$h(x,y) = \int_{-\infty}^{+\infty} \int f(\alpha,\beta) \cdot g(x-\alpha, y-\beta) d\alpha d\beta \quad (3)$$

where $f(\alpha,\beta)$ is the input signal (= image), $h(x,y)$ the output signal (transformed image) and $g(x-\alpha, y-\beta)$ the response of the transformation system (optical or electronical, see BÄHR 1985). This basic equation, the convolution integral, may be simplified for the frequency domain:

$$H(u,v) = F(u,v) \cdot G(u,v) \quad (4)$$

After Fourier Transformation of the parameters, $G(u,v)$ is the transformation function ("spread function") for the input spectrum $F(u,v)$. Its absolute values represent the MTF:

$$\text{MTF} = |G(u,v)| \quad (5)$$

Obviously, this equation seems useful to determine the MTF. For measuring purposes the adequate object is an edge in the output image. An edge contains all frequencies and will therefore result in a complete MTF.

Many authors describe this method or other approaches for computing (5) (e.g. FRANKE 1964; SIEVERS 1976; FANG LEI, TIZIANI 1988). We have used the graph of an edge profile as it is shown in Fig 4. The sequence for computing the MTF is:

1. Edge profile measured from high contrast bar target
2. Differentiation of the profile leads to the spread function
3. Absolute values of the Fourier transformed spread function compose the MTF

This procedure differs in two respects from the given formulas:

In practice we have discrete functions and therefore sums instead of integrals. Furthermore the edge approach is in one dimension, which turns the v parameter obsolete.

The described approach was developed for conventional lens/film-systems, but it is perfectly suitable for digital cameras, too. This is because in general a computer based dialog system and a monitor are involved so that the 3 steps may be performed on-line. Computing time on the PDP 11/73 for 1 MTF is less than 1 s; the complete process including I/O is 5.4 s.

The results obtained from the edge gradient analysis are identical to those obtained by the direct method for 3-bar- targets.

Consequently, the MTF curves presented in FIG.3 have been derived exactly with the same result from the EGA, too. This proves the agreement of both methods and is of great importance: For practical applications the EGA seems more feasible because it derives from a single profile, whereas the direct method affords a particular profile for each frequency. Beside this, in imagery from aerial or space platforms it is nearly impossible to find appropriate targets for the different frequencies. The probability for detecting useful **edges** is higher, anyway.

The simple EGA allows to test the image quality in many respects without great efforts. FIG.5 shows the aperture effect of the lens system. The loss of resolving power for larger apertures is due to deterioration of the lens system. The light-fall-off, another optical parameter which affects the image quality, was not observed. This is because the sensor plane uses only the central part of the projected image ($f = 12.5 \text{ mm}$ and 8.0 mm). Errors of the EGA for MTF determination have been found for

$$m_{\text{MTF}} = \pm 0,04$$

(internal accuracy from repeated measurements at different edges). The main error source is the noise in the electronical system. The influence of this effect can be reduced by repeating profile measurements and taking mean values.

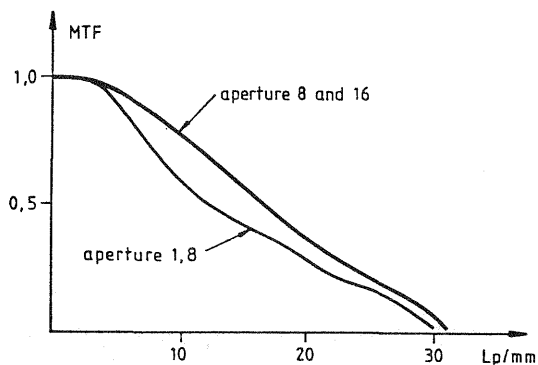


FIG. 5: MTF from EGA for different lens apertures (vertical direction)

3.3 Pointing Accuracy from Digital Correlation Procedure (DCP)

The MTF is a fundamental quantity for describing the geometrical resolution of imaging systems. However, these systems are used for carrying out practical tasks, and the effect of the resolving power on the results should be known. In this paragraph the question is:

"What is the impact of geometrical resolution on pointing accuracy for a digital camera?"

Measuring single points is a standard task in photogrammetry. In order to isolate the effect of system resolution, the influence of signals or subjective measurements had to be eliminated. Therefore the investigation was done for ideal, artificial signals by digital correlation.

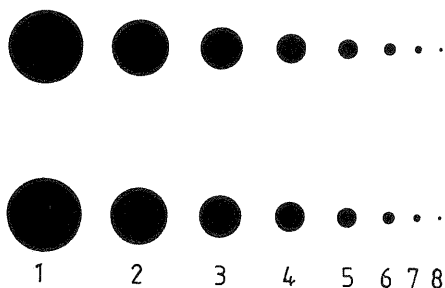


FIG. 6: Configuration of signals as taken by the camera, reduced by factor 4 from original size

FIG.6 shows the configuration of the signals as they were taken by the digital camera. Two parallel rows were prepared containing circular signals ranging from 40 mm diameter down to below 1 mm. For correlation, the 2 rows in FIG.6 are available (case A). Beside this, another image was taken from the same test figure, observing a slightly different orientation, thus allowing correlation of similar rows but different images (case B). This leads to the following alternatives for correlation:

		Image A:		Image B:	
		Right row	Left row	Right row	Left row
Image A:	Right row		ArAl		
	Left row				AlBl

Table 2: Possibilities for the DCP (r: right; l: left)

The two indicated cases, ArAl and AlBl, will be discussed now.

The varying diameter of the circles simulates varying resolution. Instead of changing distance, the basic relation "pixels per signal" was achieved by this means. For correlation, only the peripheral pixels of the circles ("mixed pixels" = "mixels") contribute to the result. The number of these pixels may be computed a priori from

$$P_p = 2k \sqrt{\pi F} \quad (\text{BÄHR 1984}) \quad (6)$$

where F is the area surface, k the shape parameter and Pp the number of peripheral pixels. This general formula reduces to

$$P_p = 2\pi r \quad (7)$$

for circular areas with a radius of r pixels. The values determined from (6) and (7) are theoretical values, modelling the edges of the signals mathematically.

For correlation the most precise procedure available was taken, i.e. the least squares approach as it is implemented in Karlsruhe (PIECHEL 1986). In order to reach its full potential, excellent approximate values have to be introduced. Therefore, the DCP is done stepwise:

- 1.) Determination of the cross correlation coefficient
- 2.) Approximation by parabolic curves in both directions
- 3.) Least squares correlation

The final results are presented in Table 3. The input data are mean values from 4 images for reduction of noise. The following observations are made:

- 1.) Best precision is in the order of 1/100 pixel
- 2.) Correlation in y (perpendicular to line direction) is in all cases 10...20% better than correlation in x (in line direction). This is due to the sensor element shape and was expected according to paragraph 2 and 3.2.

- 3.) Case AlBl gives better results than ArAl. Two reasons may contribute to this fact: differences in the (manually drawn) circles of the two rows and irregularities of the drawing film surface, causing different reflections for the two different rows.
- 4.) The obtained precision is a function of the involved number of peripheral pixels. From 97 to 27 pixels loss of accuracy is not significant. For less than 10 peripheral pixels the results are no longer acceptable.

Signal number	Diameter (mm) (= signal)	Diameter d (Pix) (= image)	Periph. Pixels (numbers)	Window (Pix)	Residuals (Pix)			
					Case ArAl x (horizontal)	Case ArAl y (vertical)	Case AlBl x (horizontal)	Case AlBl y (vertical)
1	40	31	97	39	0,012	0,011	0,008	0,007
2	31	24	75	31	0,013	0,012	0,009	0,008
3	23	18	56	25	0,012	0,010	0,010	0,009
4	16	12,5	39	25	0,012	0,011	0,012	0,011
5	11	8,5	27	17	0,015	0,013	0,014	0,012
6	7	5,5	17	17	0,024	0,019	0,021	0,017
7	4	3	9	11	0,041	0,029	0,031	0,024
8	2	1,5	5	11	0,123	0,090	0,147	0,097
9	0,4	0,3	1	11	0,185	0,121	--	--

Table 3: Results from DCP. Residuals are mean square errors

The window size does not change the results. For signal 9 the results remain "unstable" when taking smaller windows. If a signal falls completely into 1 pixel, we have the case discussed in (BAHR 1976), which theoretically yields a mean precision of +/- 1/3 pixel.

The DCP applied allows only shifting in x and y direction. If a scale factor is introduced in addition, it does not change the result, which proves that the simpler model is satisfactory. If only 1 image is used instead of the mean values of 4, the results are highly affected by noise, and the residuals are considerably larger (10...50%).

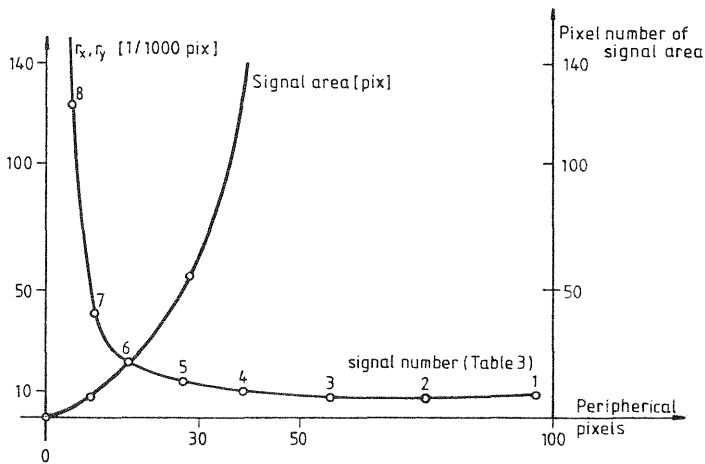


FIG. 7: Residuals as a function of peripheral pixels involved in the DCP

FIG.7 shows the dependency of residuals after the DCP in function of the number of involved peripheral pixels. If we take the pixel size (PS) for "resolution", the achieved maximum pointing accuracy (PA) of the digital camera is simply expressed by:

$$PA_{max} \sim \frac{PS}{100} \quad (8)$$

This is true for signal 1 (750 pixels involved) down to signal 4 (120 pixels involved), i.e. independent from the geometrical resolution. The results are tolerable down to the threshold, where the number of peripheral pixels is equal to the number of pixels involved in the signal area, which is the case for $P_p = 12$:

$$PA_{min} = 3PA_{max} \text{ for } d = 4PS \quad (9)$$

Below this value the geometric resolution will not be tolerable any more for pointing purposes.

We have to observe that the results are based on the internal accuracy of the DCP and are valid only for the used HITACHI/VTE camera system. The basic results of this empirical investigation, however, will be confirmed for digital cameras in general.

3.4 Interpretability from Digitized Aerial Photography

This again is a standard task in photogrammetry, but difficult to define rigorously, in contrast to the pointing accuracy. For testing purposes a conventional aerial photo (23 cm x 23 cm, c = 152 mm) was taken, showing the center of the city of Karlsruhe / FRG (see FIG.8). In this paragraph the question will be as follows:

"What is the impact of geometrical resolution on the interpretability of a conventional scene for a digital camera?"

For this purpose the transparency of the photography was registered by the digital camera system. The available field of 512 by 512 pixels was matched to the peripheral road of Karlsruhe, of 2200 m diameter, with the castle in the center. Hence 1 pixel in the image corresponds to $2200 \text{ m} / 512 = 4.3 \text{ m}$. One has to point out that this value does not allow to conserve the resolution of the original image, which was determined to be around 40 Lp/mm. This leads to 0,9 m for 1 Lp at the ground, which theoretically is an order of magnitude better than 4.3 m pixel size.

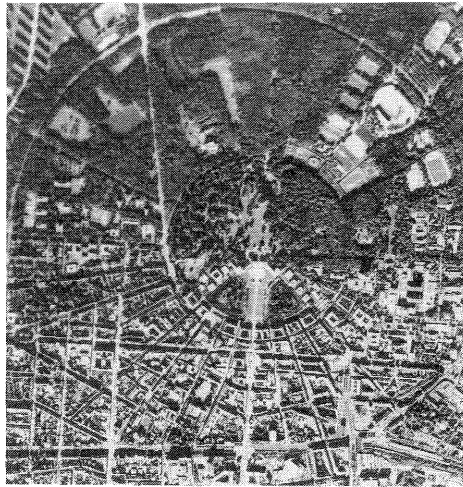


FIG. 8: Section of the analysed aerial photography. Original size, scale 1 : 36.000, oriented to the north.
 Photo taken October 19, 1987
 Clearance: 483/88 of March 2, 1988
 Center: Karlsruhe Castle. East: University Campus;
 Northeast: Sport Installations; South: City Center
 Courtesy of HANSA LUFTBILD Company, MÜNSTER/FRG.

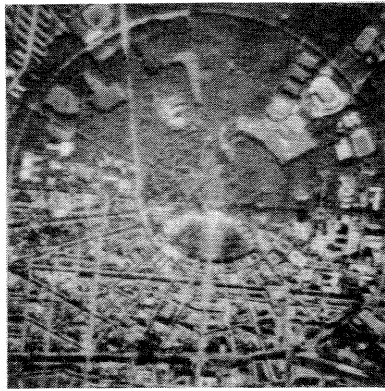
For analysing the effect on interpretability, pixels had to be magnified. This is principally possible in two ways:

1. taking the photographs by the digital camera from larger distances (including a zoom), or
2. adding pixels digitally.

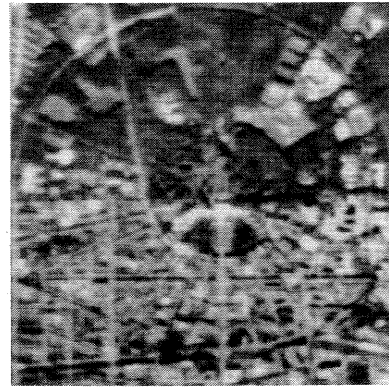
FIG.9 demonstrates the results. For both approaches the pixel size changes from 100 μ (9a = original) to 800 μ (9d and 9g). Referring the pixel size to the ground, the loss of resolution is evident only for the first approach, ranging from 4.3 m (a) over 8.6 m (9b) and 17.2 m (9c) to 34,4 m (9d), whereas the pixel size on the ground of course remains constant (i.e.4.3 m) for 9e. Consequently, the analysis of interpretability has to be restricted to FIG.8 and the cases a, b, c and d of FIG.9.

Object	Dimension approx.	Threshold for Detection (Pixel Size)	FIG.
Single Trees	5m...10m	4.3m	9a
Forest Type	-	8.6m	9b
Large Buildings	30m x 50m	8.6m	9b,c
Minor Roads	20m	4.3m...8.6m	9b
Mayor Roads	40m	34.4m	9c
Sport Fields	100m...350m	17.2m	9d

Table 4: Interpretability of different objects in FIG.9



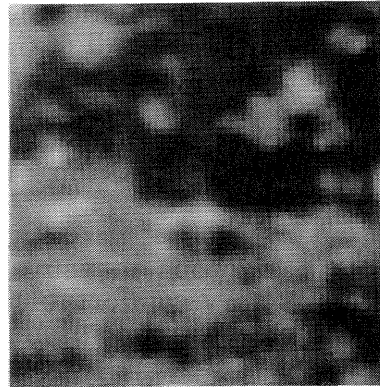
a



b



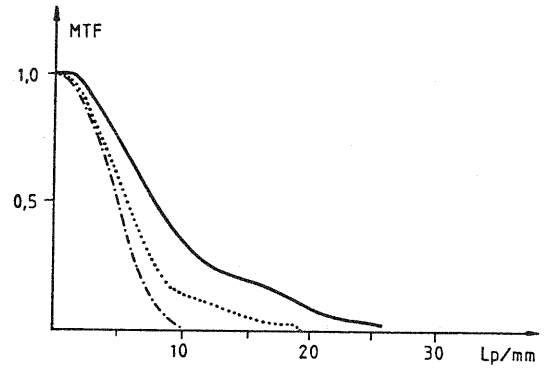
c



d



e



f

FIG. 9: Variation of interpretability

a: Best resolution for digital camera image (100 μm 4,3 m)

b: Distance Factor 2 (100 μm 8,6 m)

c: Distance Factor 4 (100 μm 17,2 m)

d: Distance Factor 8 (100 μm 34,4 m)

e: Digital adding of pixels (Factor 2)

f: MTF curves

case a: Solid line

case b: Dashed line

case c: Dotted line

The table resumes the interpretability/detectability for different objects. The relatively bad result may partially be due to a defocussing effect of the digital camera system. Moreover, the reproductions presented in FIG.8 and 9 are far from the quality of the originals. In the visual test the effect from horizontal/vertical direction was not noted.

The interpretability of image objects can not be represented by a simple function of geometric resolution as it is possible for pointing purposes of well-defined targets. The conditions for interpretability of course are more complex. The detectability for edges of high contrast is below pixel size, but for object recognition the object has to be composed of several pixels. The number depends on the object shape and is in the order of 2...3 pixel size in both directions (see Table 4).

4. Conclusions

Although digital cameras include optical components and consequently form a hybrid system, the specific digital process of image formation plays a fundamental role for geometric resolution: Size of the sensor cells is not equal to pixel size because of completely different A/D conversion in both directions. The final MTF still shows clearly these effects. Geometric resolution was found to be a function of horizontal or vertical direction and of contrast, free from position effects of the sensor chip.

The MTF is a rigorous measure for geometric resolution. Its determination by digital means is very comfortable when using the Edge Gradient Analysis (EGA). For digital camera systems automatic implementation is possible, and visual means become obsolete. Internal precision for MTF determination is around +/- 0.04, electronical noise providing the main component.

The MTF is not very illustrative as far as its significance for specific applications is concerned. This is shown first for pointing accuracy, applying digital correlation procedures (DCP) at circular artificial targets. **The result does not depend on geometric resolution (pixel size) within a certain range.** Target diameters resolved from 30 pixels down to 12 pixels yield constant residuals around +/- 1/100 pixels, for vertical direction 10...20% better than for horizontal direction. Limiting factors are electronical noise as well as the number of peripheral pixels involved in the DCP.

Interpretability, on the other hand, is an application for which resolution effects show a completely different impact as for pointing accuracy. For detection and recognition of objects these objects generally have to be composed of several pixels. A building of 30m x 30m, for instance, affords 3x3 pixels of about 10 m size on the ground and good contrast to be visually recognized. The same resolution may provide a pointing accuracy of +/- 10 cm for ideal targets. This discrepancy demonstrates that geometric resolution should not be considered as an isolated parameter. System characteristics like MTF, LP/mm or pixel size have to be referred to the respective task for being adequately employed.

Acknowledgements

I would like to thank Dipl.-Ing. J. Piechel and Dipl.-Ing. T. Vögtle at Karlsruhe Institute for Photogrammetry and Remote Sensing for providing the data of the DCP and the MTF, as well as HANSA LUFTBILD Company for fruitful collaboration.

REFERENCES

- ACKERMANN, F.: High Precision Digital Image Correlation. 39. Photogrammetric Week, Stuttgart 1984
- ACKERMANN, F.: Digital Image Correlation: Performance and Potential Application in Photogrammetry. Photogrammetric Record, 1984, p.429-439
- BÄHR, H.P.: Analyse der Geometrie auf Photodetektoren abgetasteter Aufnahmen von Erderkundungssatelliten. Wissenschaftliche Arbeiten der Fachrichtung Vermessungswesen der Universität Hannover Nr. 71, Hannover 1976
- Bähr, H.P.: Wechselwirkung von Photogrammetrie und Fernerkundung durch Anwendung digitaler Bildverarbeitung. Wissenschaftliche Arbeiten der Fachrichtung Vermessungswesen der Universität Hannover Nr. 97, Hannover 1979
- BÄHR, H.P.: Abschätzung einiger geometrischer Fehlerkomponenten bei der multispektralen Klassifizierung. Bildmessung und Luftbildwesen (52) 1984, p.23-29
- BÄHR, H.P.:
(Hrsg.) Digitale Bildverarbeitung - Anwendung in Photogrammetrie und Fernerkundung. Wichmann-Verlag Karlsruhe 1985
- DÄHLER, J. Problems in Digital Image Acquisition with CCD cameras. ISPRS Intercommission Conference on Fast Processing of Photogrammetric Data, Interlaken 1987.
- DUCHER, G. Panorama de la participation de l'IGN au projet de prises de vues SPACELAB. ESA Metric Camera Workshop, DFVLR Oberpfaffenhofen 1985
- FANG LEI,
TIZIANI, H.J.: A Comparison of Methods to Measure the Modulation Transfer Function of Aerial Survey Lens Systems from the Image Structures. Photogrammetric Engineering 1988, p.41-46.
- FRANKE, G.: Photographische Optik. Akademische Verlagsgesellschaft, Frankfurt 1964
- HOFMANN, O. Dynamische Photogrammetrie. Bildmessung und Luftbildwesen (54) 1986, p.105-121
- KONECNY, G.,
BÄHR, H.P.,
REIL, W.,
SCHREIBER, C.: Einsatz photogrammetrischer Kameras aus dem Weltraum für kartographische Anwendungen. Institut für Photogrammetrie und Ingenieurvermessungen Universität Hannover, 1979
- KONECNY, G., Investigation of Interpretability of Images

- SCHUHR, W.
Wu, J.: by Different Sensors and Platforms for Small Scale Mapping. ISPRS Comm.I Symposium, Canberra 1982
- PIECHEL, J.: Investigations of Different Interest Operators for DTM-Generation by Epipolar Line Correlation. ISPRS Comm.III Symposium, Rovaniemi 1986
- SIEVERS, J.,
RUTHOTTO, H. Quality Analysis Methods for Spacelab Mission Film Selection. ISPRS Comm.I, Hamburg 1980
- SIEVERS, J.: Die Kantenbildanalyse als Mittel zur Bestimmung von Bildparametern. Working Group E of OEEPE, 1976.
- TOGLIATTI, G.V. Quality Analysis Methods Selecting Film Material for the First Spacelab Mission 1. ISPRS Comm.I, Hamburg 1980
- VÖGTLE, T.,
WIESEL, J. Evaluation of a Solid State Camera for Photogrammetric Applications. ISPRS Comm.I Symposium, Stuttgart 1986.
- WELCH, R.: Image Quality Requirements for Mapping from Satellite Data. ISPRS Comm. I Symposium, Canberra 1982
- ZIEMANN, H.: Optical Transfer Functions as Image Quality Measure in Photogrammetry. International Scientific Colloquium, Leipzig 1987